

# Glass-like recovery of antiferromagnetic spin ordering and dimensional crossover in a photo-excited manganite $\text{Pr}_{0.7}\text{Ca}_{0.3}\text{MnO}_3$ compound using ultrafast x-ray scattering spectroscopy

S.Y. Zhou,<sup>1,2,3,\*</sup> Y. Zhu,<sup>1,4</sup> M.C. Langner,<sup>1</sup> Y.-D. Chuang,<sup>2,\*</sup> T.E. Glover,<sup>2</sup> M.P. Hertlein,<sup>2</sup> A.G. Cruz Gonzalez,<sup>2</sup> N. Tahir,<sup>2,5</sup> Y. Tomioka,<sup>6</sup> Y. Tokura,<sup>7,8</sup> D.-H. Lee,<sup>1</sup> Z. Hussain,<sup>2</sup> and R.W. Schoenlein<sup>1,\*</sup>

<sup>1</sup>*Materials Sciences Division, Lawrence Berkeley National Laboratory, Berkeley, CA 94720, USA*

<sup>2</sup>*Advanced Light Source, Lawrence Berkeley National Laboratory, Berkeley, CA 94720, USA*

<sup>3</sup>*State Key Laboratory of Low Dimensional Quantum Physics and Department of Physics, Tsinghua University, Beijing 100084, China*

<sup>4</sup>*Department of Applied Science, University of California, Davis, CA 95616, USA*

<sup>5</sup>*National Center for Physics, Islamabad, Pakistan*

<sup>6</sup>*Nanoelectronics Research Institute, National Institute of Advanced Industrial Science and Technology (AIST) Tsukuba Central 4, 1-1-1 Higashi Tsukuba 305-8562, Japan*

<sup>7</sup>*Department of Applied Physics, University of Tokyo, Bunkyo-ku, Tokyo 113-8656, Japan*

<sup>8</sup>*Cross-Correlated Materials Research Group (CMRG) and Correlated Electron Research Group (CERG), Advanced Science Institute, RIKEN, Wako 351-0198, Japan*

(Dated: September 18, 2012)

**Time-resolved resonant soft x-ray scattering spectroscopy reveals the glass-like physics that mediates the dynamics of antiferromagnetic spin ordering in a transient photo-excited  $\text{Pr}_{0.7}\text{Ca}_{0.3}\text{MnO}_3$  manganite. The evolution of spin ordering, measured nearly 12 decades in time (70 ps to tens of seconds), exhibits an unambiguous stretched-exponential behavior that is a hallmark of glass-like systems. Moreover, a dimensional crossover in the effective interaction from 1D at low pump fluence to 3D at high pump fluence is observed, suggesting that spin ordering and orbital ordering are transiently decoupled by photo-excitation.**

Nanoscale electronic orderings of charges, orbitals and spins (e.g. into stripe or checkerboard patterns) are observed in many strongly correlated electron materials, and the competing ground states associated with these ordered phases underlie important emergent material properties, such as colossal magnetoresistance (CMR) [1, 2], high temperature superconductivity [3], and multi-ferroic behavior [4]. Understanding the fundamental origin of these phases and the dynamic interplay between them remain important scientific challenges. Transient photo-excitation is an effective means for separating the strong coupling of electron, lattice, orbital and spin degrees of freedom based on their time response and can drive transitions between competing states, e.g. photo-induced transient insulator-metal transition (IMT) in charge/orbital/spin ordered CMR manganites [5, 6], and transient superconductivity in a stripe-ordered cuprate [7]. Moreover, transient excitations can be used to create metastable phases from which the re-establishment of the ordered states may be directly observed via ultrafast probes. Incorporating time-resolved resonant soft x-ray scattering spectroscopy (TR-RSXS) as an ultrafast probe [8–12] fills a critical knowledge gap by providing detailed information on the spatial ordering of charges, orbitals and spins, and how these ordered phases develop and evolve in response to tailored perturbations - information

that is not available from either static or time-resolved optical probes [13, 14], or x-ray absorption spectroscopy (XAS) [15], or transport measurements [5, 6].

TR-RSXS research to date [8–12] has focused on the ultrafast frustration or “melting” of electronic ordering within the first 100 ps following photo-excitation, however, the reverse process, i.e. “re-establishment” of such ordering, has been heavily overlooked. In this letter, we focus for the first time on the re-establishment of electronic ordering from a metastable phase. Using TR-RSXS to follow the antiferromagnetic spin ordering (SO) in a photo-excited  $\text{Pr}_{0.7}\text{Ca}_{0.3}\text{MnO}_3$  [16] over an unprecedented temporal window spanning 12 decades, we identify an unambiguous stretched-exponential behavior that is a hallmark of glass-like systems. This is in striking contrast to the response of charge carriers which is dominated by electron or lattice interactions with recovery time shorter than 100 ps [17]. Moreover, we report a dimensional crossover in the effective interaction from 1D at low pump fluence to 3D at high pump fluence, which suggests that spin ordering and orbital ordering (OO) can be transiently decoupled by photo-excitation. Our results not only challenge presumptions about photo-excitation of electronic orderings but also provide a new perspective for revealing the fundamental physics underlying such electronic self-assembly phenomena.

TR-RSXS experiments were carried out at the ultrafast soft x-ray Beamline 6.0.2 of the Advanced Light Source (ALS), Lawrence Berkeley National Laboratory. Previous static RSXS studies showed that the (1/4, 1/4, 0) superlattice diffraction peak (in pseudocubic notation)

\*Correspondence should be sent to syzhou@phys.tsinghua.edu.cn, YChuang@lbl.gov and rwschoenlein@lbl.gov.

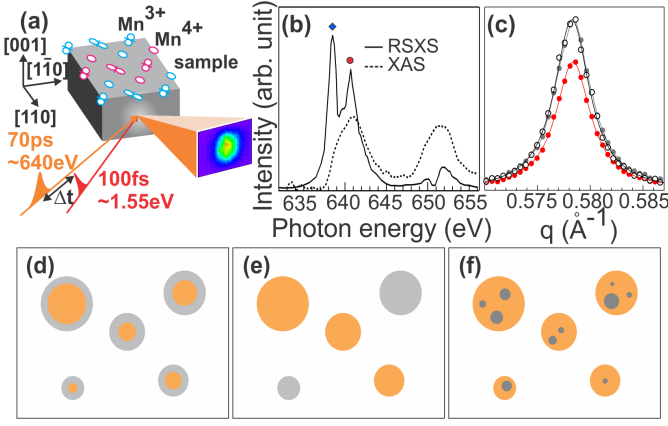


FIG. 1: (a) Schematic diagram of the CE-type SO state overlaid with the experimental geometry for TR-RSXS measurements. Circles and lobes represent the Mn<sup>4+</sup> sites and e<sub>g</sub> orbitals on the Mn<sup>3+</sup> sites. Pink and blue colors represent opposite spin orientations. (b) Energy profile of the SO diffraction peak from static RSXS measurements (solid line) as compared to the XAS spectrum (dotted line) [19]. The symbols mark the photon energies used. (c) Comparison of the SO diffraction peak intensity measured at 641.4 eV before (open circles) and  $\Delta t=500$  ps after laser excitation at 1 mJ/cm<sup>2</sup> pump fluence (red filled circles). Solid lines are fits using Lorentzian function. Gray circles are data taken at  $\Delta t=500$  ps rescaled by a factor of 1.33. (d-f) Schematic plots showing three possible responses of SO domains to photo-excitation. The orange areas represent the SO domains and the gray areas represent the regions destroyed by photo-excitation. These are oversimplified illustrations and a realistic picture is likely more complicated due to the irregular shapes and interconnections between SO domains.

at 65 K was dominated by the CE-type [18] SO state (see Fig. 1(b) for a characteristic RSXS energy profile) [19], and we focus on its dynamics in the current study. An 800 nm pump laser pulse with 100 fs duration was used to induce an IMT [5], and a 70 ps x-ray pulse was used subsequently to capture snapshots of the evolving SO. A schematic experimental geometry is shown in Fig. 1(a) and more details can be found in supplementary information. The measurement temperature was 65 K, low enough to avoid any laser-heating induced thermal phase transition.

Figure 1(c) shows the comparison of the SO diffraction peak profile as a function of momentum transfer ( $q$ ) without photo-excitation (open symbols) and at a delay time  $\Delta t=500$  ps (red filled symbols) after photo-excitation. The pump fluence is 1 mJ/cm<sup>2</sup> and the photon energy of the probe x-ray beam is tuned to Mn L<sub>3</sub> edge at 641.4 eV (red symbol in Fig. 1(b)). A reduction of the SO peak intensity is observed at  $\Delta t=500$  ps. However, the peak position and width show negligible change upon photo-excitation, which can be clearly seen after rescaling the peak profile by the intensity ratio (filled gray symbols). A Lorentzian function fit

to the data (solid lines in Fig. 1(c)) shows that the correlation length  $\xi$  ( $\xi=2\pi/\Delta q$  where  $\Delta q$  is the peak width) remains  $1560 \text{ \AA} \pm 30 \text{ \AA}$  even following suppression of the SO via photo-excitation. The negligible change in correlation length rules out the nucleation type recovery behavior illustrated in Fig. 1(d). This photo-excitation response is in striking contrast to the  $\approx 10$  times change in the SO correlation length, which is observed across the canted-antiferromagnetic transition temperature  $T_{CA}$  [19]. There are two remaining possible scenarios consistent with the negligible change of correlation length: full destroy of some SO domains without affecting other domains (Fig. 1(e)), or photo-induced local spin frustration within the SO domains (Fig. 1(f)).

Figure 2 shows the evolution of SO diffraction peak intensity as a function of  $\Delta t$ . The differential intensity, defined as  $\Delta I/I_s = (I_{\Delta t} - I_s)/I_s$  where  $I_s$  and  $I_{\Delta t}$  are the peak intensity recorded without photo-excitation and at  $\Delta t$  after photo-excitation, exhibits a step-like decrease at  $\Delta t=0$  with a fall time of 70 ps (Fig. 2(a)), which is limited by the pulse duration of the probe x-ray beam. Here we focus on the recovery dynamics at later delay time.

Figures 2(b-c) show the recovery of SO in different temporal windows. Although a bi-exponential function  $a_1 e^{-t/\tau_1} + a_2 e^{-t/\tau_2}$  with  $\tau_1 \approx 10$  ns and  $\tau_2 \approx 100$  ns seems to give a reasonable description of the data within the first 80 ns (solid lines in Fig. 2(b)), a clear discrepancy is evident in the  $\mu s$  regime (Fig. 2(c)), suggesting that more exponential functions are needed to fit the entire curve. In fact, the number of exponentials needed depends strongly on the selected temporal window and this reflects the inadequacy of using a multi-exponential function fit. The observed recovery behavior does not depend on the photon energies of the probe x-ray beam (red circles vs. blue diamonds), although different photon energies lead to variations in the probe depth [20] and differential signal. The recovery process not only involves multiple time scales, but also strongly depends on the pump fluence. Figures 2(d-g) show the recovery of SO with increasing pump fluence. The full recovery time increases rapidly from sub- $\mu s$  at low pump fluences (Fig. 2(d)) to tens of seconds at higher pump fluences (Fig. 2(g)). The surprisingly long recovery time rules out conventional electronic or lattice interactions which typically have recovery time shorter than 100 ps [17] as the dominant recovery mechanism. The strong pump fluence dependent recovery time excludes scenario illustrated in Fig. 1(e), since if SO domains are destroyed and recovered uncorrelated to each other, the recovery time is not expected to show such strong pump fluence dependence.

The large temporal range and the strong fluence dependence in the recovery process are commonly seen in glass-like or complex disordered systems [21], such as structural glass [22], magnetic glass [23] etc. In such systems, the dynamics can be described by the stretched-exponential function (Kohlrausch-Williams-Watt function) in the form of  $a_1 e^{-(t/\tau)^\beta}$  [21]. Remarkably, with

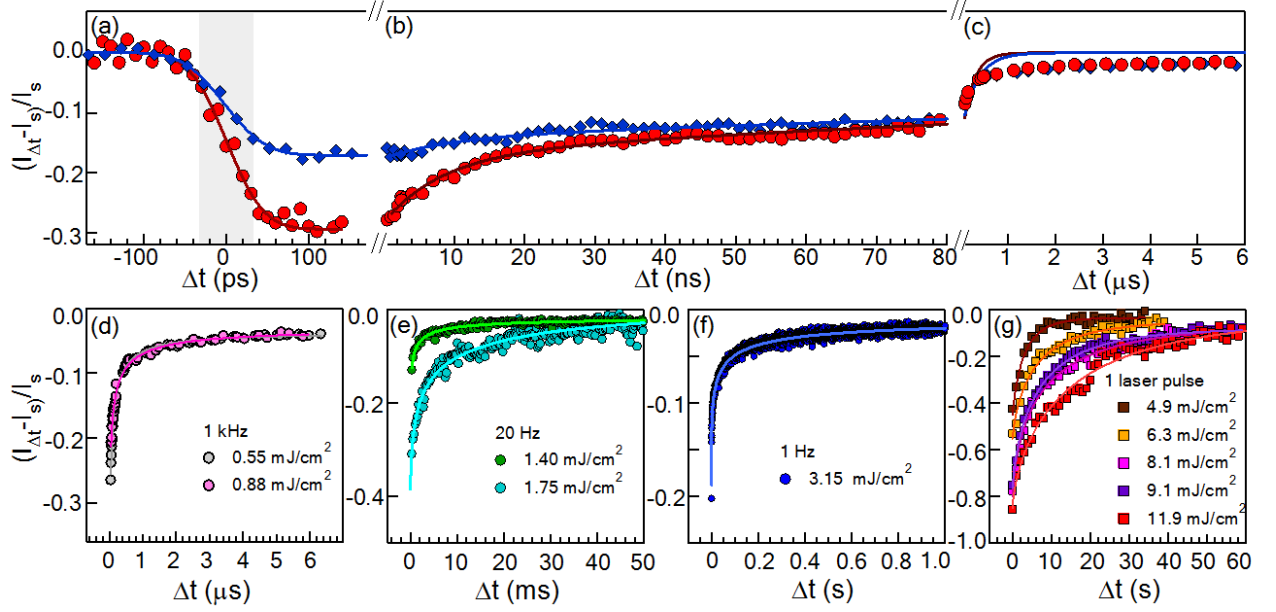


FIG. 2: (a-c) Differential SO peak intensity measured at 641.4 eV (red circles) and 639.2 eV (blue diamonds) as a function of pump-probe delay time  $\Delta t$  at  $1 \text{ mJ/cm}^2$  pump fluence. The solid lines in panel (a) are fits using the error function and the shaded area marks the 70 ps temporal resolution of probe x-ray beam. The bi-exponential function fits up to 80 ns are shown as solid lines in panels (b) and (c). (d-g) Differential SO peak intensity as a function of delay time with different pump fluences. Symbols are raw data and solid lines are the stretched-exponential function fits. The repetition rate of 800 nm pump beam, listed in each panel, is reduced at high pump fluences to ensure that the sample is fully recovered before the arrival of next pump pulse.

only three adjustable parameters,  $a_1$ ,  $\tau$  and  $\beta$ , an excellent agreement between data (symbols in Figs. 2(d-g)) and the stretched-exponential function fits (lines) is achieved over entire 12 decades of measurement temporal window. This strongly points to the glass-like nature in the recovery process of photo-excited SO state.

It is surprising that the recovery of the long-ranged periodic SO shares similar dynamics to glass-like systems which are typically highly disordered. Based on the invariance of correlation length and the glass-like dynamics, we propose a microscopic picture in which photo-excitation creates local spin frustrations within the SO domains (Fig. 1(f)). The spin frustrated regions are sufficiently small that they do not affect the overall domain size, or the correlation length of SO across the domains. Restoring these frustrated spins with different sizes can lead to the observed glass-like behavior. Interestingly, TR-RSXS data on  $\text{Pr}_{0.5}\text{Ca}_{0.5}\text{MnO}_3$  with low temperature robust charge/orbital/spin ordered ground states does not show clear glass-like behavior even at a pump fluence of  $6 \text{ mJ/cm}^2$  (see supplementary information). The proximity of different ground states in  $\text{Pr}_{0.7}\text{Ca}_{0.3}\text{MnO}_3$  but not in  $\text{Pr}_{0.5}\text{Ca}_{0.5}\text{MnO}_3$  [16] further supports the glass-like behavior observed in  $\text{Pr}_{0.7}\text{Ca}_{0.3}\text{MnO}_3$  because frustration is an indispensable ingredient for glass-like systems [1]. We note that although various types of glass-like behavior have been reported in manganites, e.g. spin glass [24, 25], clus-

ter glass [26], polaron glass [27], strain glass [28, 29] etc, those are intrinsic properties of the ground states revealed by static measurements. Our TR-RSXS work reveals dynamic signatures of glass-like behavior in the long-ranged ( $\xi \approx 1500 \text{ \AA}$ ) SO after photo-excitation, and its transient glass-like behavior is fundamentally different from the short ranged spin glass (negligible  $\xi$ ) or polaron glass ( $\xi \leq 10 \text{ nm}$ ) [27, 30] previously discussed in the equilibrium state of manganites.

In addition to revealing novel glass-like dynamics, the effective dimensionality  $d$  of the interaction that restores SO can be retrieved from the stretched-exponent  $\beta$  via the relationship  $\beta = d/(d+2)$ . Renormalizing the time traces in Figs. 2(d-g) by  $a_1$  and  $\tau$  leads to two universal groups: data with pump fluences below and above  $4 \text{ mJ/cm}^2$  are in overall agreement with  $\beta=1/3$  ( $d=1$ ) and  $\beta=3/5$  ( $d=3$ ) respectively. The abrupt jump around  $4 \text{ mJ/cm}^2$  in  $\beta$  (Fig. 3(b)) implies a dimensional crossover from 1D to 3D in the effective interactions that are responsible for the restoration of the SO. We note that while dimensional crossover has been reported in many systems by tuning thermodynamic variables under equilibrium conditions [31], our results represent its manifestation in a dynamic regime. A likely scenario for the observed 1D recovery dynamics at low pump fluence is that the OO remains largely intact even though the SO is disturbed by photo-excitation. The intra-chain interaction along the quasi-1D OO path provides the restoring

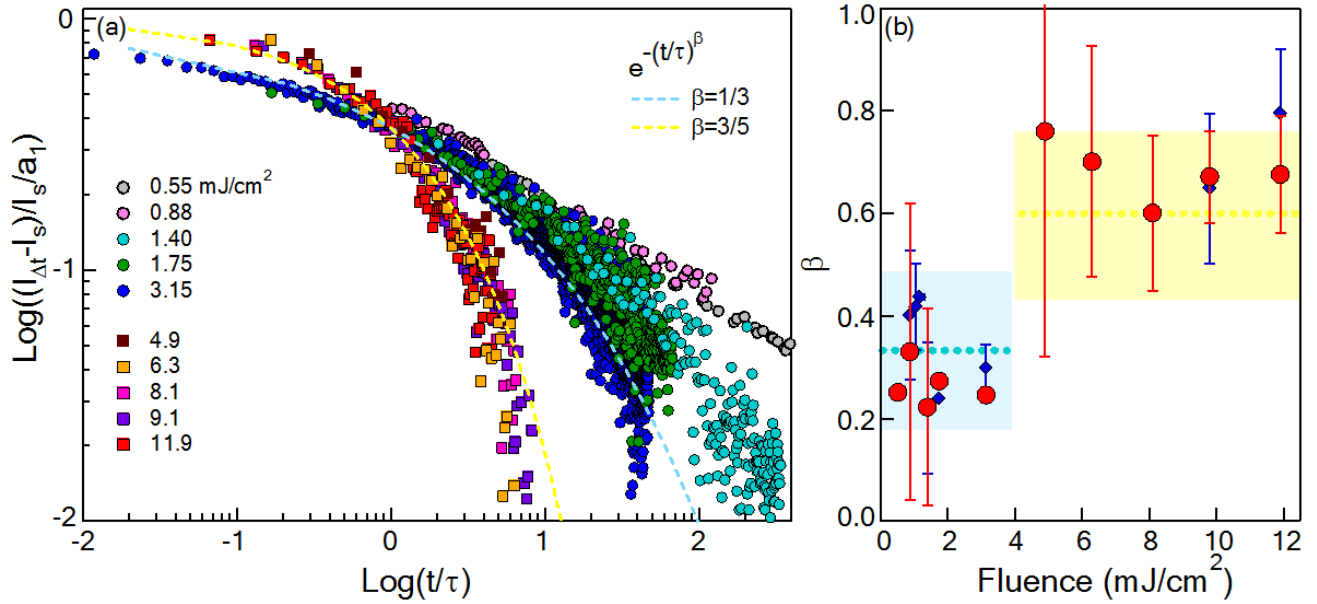


FIG. 3: (a) Log-Log plot of data shown in Figs. 2(d-g). The differential signal and time scale are normalized by  $a_1$  and  $\tau$  extracted from the stretched-exponential function fit respectively. The dashed cyan and yellow lines represent the stretched-exponential functions with  $\beta=1/3$  and  $\beta=3/5$ . (b) The stretched exponent  $\beta$  and error bar extracted from the stretched-exponential function fit as a function of pump fluence. The shaded areas and dotted lines are guides for the eyes. Red circles and blue diamonds are data measured at photon energies of 641.4 eV and 639.2 eV respectively.

force for SO based on Goodenough-Kanamori rules [32]. Therefore the observed dimensional crossover suggests an interesting possibility that despite the intimate coupling of spin and orbital degrees in the static ordered state, the SO and OO may be transiently decoupled in their response to ultrafast photo-excitation.

In summary, our TR-RSXS studies of SO dynamics covering 12 decades in time show that the SO recovery dynamics exhibits glass-like behavior with a dimensional crossover from 1D to 3D. Our work provides a new perspective for revealing the fascinating physics hidden in the heavily overlooked recovery process of electronic orderings in many other correlated materials. For example, similar studies on the recovery dynamics of stripe may shed new light on the physics involved in photo-induced

superconductivity [7].

### Acknowledgments

We thank H. Yao and W.L. Yang for useful discussions. This work was supported by the Director, Office of Science, Office of Basic Energy Sciences, the Materials Sciences and Engineering Division under the Department of Energy Contract No. DE-AC02-05CH11231. The Advanced Light Source is supported by the Director, Office of Science, Office of Basic Energy Sciences, of the U.S. Department of Energy under Contract No. DE-AC02-05CH11231.

- 
- [1] E. Dagotto, T. Hotta and A. Moreo, *Colossal magnetoresistant materials: the key role of phase separation*, Phys. Rep. **344**, 1 (2001).
  - [2] Y. Tokura, Rep. Prog. Phys. **69**, 797 (2006).
  - [3] J.M. Tranquada *et al.*, Nature **375**, 561-563 (1995).
  - [4] N. Ikeda *et al.*, Nature **436**, 1136 (2005).
  - [5] M. Fiebig *et al.*, Science **280**, 1925 (1998).
  - [6] Rini, M. *et al.*, Nature **449**, 72 (2007).
  - [7] D. Fausti *et al.*, Science **331**, 189 (2011).
  - [8] N. Pontius N. *et al.*, Appl. Phys. Lett. **98**, 182504 (2011).
  - [9] H. Ehrke *et al.*, Phys. Rev. Lett. **106**, 217401 (2011).
  - [10] S.L. Johnson *et al.*, Phys. Rev. Lett. **108**, 037203 (2012).
  - [11] W.S. Lee *et al.*, Nature Common. **10**, 1038 (2012).
  - [12] M. Forst *et al.*, Phys. Rev. B **84**, 241104(R) (2011).
  - [13] M. Fiebig *et al.*, Appl. Phys. Lett. **74**, 2310 (1999).
  - [14] R.I. Tobey, D. Prabhakaran, A.T. Boothroyd, A. Cavalleri, Phys. Rev. Lett. **101**, 197404 (2008).
  - [15] M. Rini, *et al.*, Phys. Rev. B **80**, 155113 (2009).
  - [16] Y. Tomioka, A. Asamitsu, H. Kuwahara, Y. Moritomo, Y. Tokura, Phys. Rev. B **53**, R1689 (1996).
  - [17] R.D. Averitt and A.J. Taylor, J. Phys.: Condens. Matter **14**, R1357-R1390 (2002).
  - [18] CE-type structure refers to a combination of C and E type spin structure [1], which consists of quasi-one dimen-

sional zigzag chains with opposite spins as schematically drawn in Fig. 1(a).

- [19] S.Y. Zhou *et al.*, Phys. Rev. Lett. **106**, 186404 (2011).
- [20] K.J. Thomas *et al.*, Phys. Rev. Lett. **92**, 237204 (2004).
- [21] J.C. Phillips, Rep. Prog. Phys. **59**, 1133 (1996).
- [22] P.G. Debenedetti and F.H. Stillinger, Nature **410**, 259 (2001).
- [23] J.M.D. Coey, D.H. Ryan, R. Buder, Phys. Rev. Lett. **58**, 385 (1987).
- [24] P. Levy, F. Parisi, L. Granja, E. Indelicato, G. Polla, Phys. Rev. Lett. **89**, 137001 (2002).
- [25] R. Mathieu, D. Akahoshi, A. Asamitsu, Y. Tomioka, Y. Tokura, Phys. Rev. Lett. **93**, 227202 (2004).
- [26] A. Maignan, C. Martin, F. Damay, B. Raveau, J. Hejtmanek, Phys. Rev. B **58**, 2758 (1998).
- [27] D.N. Argyriou *et al.*, Phys. Rev. Lett. **89**, 036401 (2002).
- [28] P.A. Sharma, S.B. Kim, T.Y. Koo, S. Guha, S.W. Cheong, Phys. Rev. B **71**, 224416 (2005).
- [29] W. Wu *et al.*, Nature Mater. **5**, 881 (2006).
- [30] J.W. Lynn *et al.*, Phys. Rev. B **76**, 014437 (2007).
- [31] T. Valla *et al.*, Nature **417**, 627 (2002).
- [32] J.B. Goodenough, Phys. Rev. B **100**, 564 (1955).